JOURNAL OF AGRICULTURAL AND FOOD CHEMISTRY

Article

pubs.acs.org/JAFC

Effects of Preslaughter Stress Levels on the Post-mortem Sarcoplasmic Proteomic Profile of Gilthead Seabream Muscle

Tomé S. Silva,*[,†,§] Odete D. Cordeiro,[†] Elisabete D. Matos,[†] Tune Wulff,[§] Jorge P. Dias,[†] Flemming Jessen,[§] and Pedro M. Rodrigues[†]

[†]CIMAR/CCMAR, Centre of Marine Sciences of Algarve, University of Algarve, Campus de Gambelas, 8005-139 Faro, Portugal

[§]DTU Food, National Food Institute, Division of Industrial Food Research, Technical University of Denmark, Søltofts Plads, Building 221, 2800 Kgs. Lyngby, Denmark

Supporting Information

ABSTRACT: Fish welfare is an important concern in aquaculture, not only due to the ethical implications but also for productivity and quality-related reasons. The purpose of this study was to track soluble proteome expression in post-mortem gilthead seabream muscle and to observe how preslaughter stress affects these post-mortem processes. For the experiment, two groups of gilthead seabream (n = 5) were subjected to distinct levels of preslaughter stress, with three muscle samples being taken from each fish. Proteins were extracted from the muscle samples, fractionated, and separated by 2DE. Protein identification was performed by MALDI-TOF-TOF MS. Analysis of the results indicates changes on several cellular pathways, with some of these changes being attributable to oxidative and proteolytic activity on sarcoplasmic proteins, together with leaking of myofibrillar proteins. These processes appear to have been hastened by preslaughter stress, confirming that it induces clear post-mortem changes in the muscle proteome of gilthead seabream.

KEYWORDS: *gilthead seabream, preslaughter stress, proteomics, post-mortem muscle, sarcoplasmic proteins*

INTRODUCTION

The gilthead seabream (*Sparus aurata*) is an important marine aquaculture species that is commercially reared in southern Europe. The most important criteria regarding aquaculture fish such as the gilthead seabream are health value, food safety, and quality (specifically, optimal organoleptic characteristics such as texture, aroma, and taste). Fish welfare is also an important factor, not only due to the ethical implications but also because there are indications that fish welfare generally promotes improved health status, higher productivities, and higher product quality criteria.[1]

Fish muscle organoleptic traits are generally multifactorial in nature: they depend on factors such as muscle cellularity, mobility of water pools, composition (fatty acid profile, salts, collagen, amino acids), myofibrillar structural integrity, and oxidative/proteolytic status. Besides that, the relative weight of these different factors on the final product quality is different between fish species, making it impossible to directly extrapolate information obtained for a single species across all.

Although some knowledge about the impact of post-mortem processes on the flesh quality of gilthead seabream is available,[2−5] it is also important to study how the preslaughter stress that aquaculture gilthead seabream is often exposed to may interact with such post-mortem processes and possibly impair fish muscle quality.

Due to the complex and multigenic nature of flesh quality traits, the use of a proteomic approach that enables the simultaneous detection of hundreds of proteins is highly beneficial, by providing a global vision on the protein content of tissues in specific physiological states. For this study, we chose to analyze specifically the sarcoplasmic fraction of gilthead seabream muscle in an attempt to maximize the number of visualized proteins (by depletion of the highly abundant myofibrillar proteins), particularly those associated with metabolic and regulatory processes.

In parallel with the proteomic analysis, several other physiological and biochemical parameters were measured,[6] which contribute to the reconstruction of a plausible model of gilthead seabream muscle degradation.

MATERIALS AND METHODS

Fish Rearing. Two groups of 32 gilthead seabream with a mean initial body weight of 473 ± 108 g were reared in 1000 L circular plastic tanks at CCMAR facilities and fed a commercial diet, once a day, until apparent satiation, reaching a final body weight of 536 ± 96 g. The seabream originated from a commercial fish farm and had been reared at CCMAR facilities during the previous 12 months. These were subjected to natural photoperiod, and seawater from Ria Formosa (37° 00′ N, 07° 56′ W) was supplied by a flow-through system (mean rearing density = 17 kg/m^3, mean temperature = 23.1 ± 1.2 °C, salinity = 37.4 ± 0.5‰) with artificial aeration (dissolved oxygen = 88 ± 11%). Prior to harvesting, fish were starved for 48 h.

Preslaughter Harvesting Stress and Sampling. For the experiment itself, two groups of five gilthead seabream (*Sparus aurata*) each were subjected to distinct levels of preslaughter stress (profound anesthesia versus net crowding for 20 min) and sacrificed by the administration of a lethal dose (270 ppm) of a water dispersible isoeugenol-based anesthetic (AQUI-S New Zealand Ltd., Lower Hutt, New Zealand; an anesthetic approved in several non-European Union

Received: January 4, 2012
Revised: August 16, 2012
Accepted: August 20, 2012
Published: August 20, 2012

countries, with a zero withdrawal period for use in fish for human consumption) to isolate the effects of preslaughter stress on flesh quality.

For the profound anesthesia condition, the water level in the tank was slowly lowered, without disturbing the fish, and AQUI-S was added to the tank (previously diluted in 1 L of salt water), for a final concentration of 60 ppm of AQUI-S. Once lethargic, fish were immediately slaughtered. For the net crowding condition, fish were confined to an extremely high density (approximately 140 kg/m^3) inside a cylindrical net, and the water level was slightly lowered until the fish became agitated. Fish were kept in this condition for approximately 20 min prior to slaughter. Three samples of the dorsal muscle were collected from each individual at distinct time points (postslaughter at 0 h, pre-rigor mortis at 6 h, and post-rigor mortis at 48 h) for a total of 30 samples.

In parallel with the proteomic analysis, several other parameters were measured for the same fish, namely, pH, lipid oxidation levels (using a thiobarbituric acid assay), collagen content (by hydroxyproline assay), sulfated glycosaminoglycan content, instrumental texture parameters, and rigor index temporal profile. A separate analysis of the nonproteomic data has already been published.[6]

Protein Extraction and Fractionation. Sarcoplasmic extracts for each of the 30 muscle samples were prepared from 200 mg of tissue, which was homogenized (Ultra Turrax T25 Basic, IKA Labortechnik) in 1.5 mL of a mild extraction buffer (50 mM Tris-HCl, pH 7.4;, 10 mM dithiothreitol (DTT), 1 mM EDTA, and a small amount of a protease inhibitor cocktail) three times for 30 s with a 30 s pause between cycles to prevent sample heating. After mechanical homogenization, a 20 min centrifugation step was performed (11200*g*, 4 °C), retaining the supernatant, which contained mostly sarcoplasmic proteins. Extracts were kept on ice or at 4 °C during the whole extraction/fractionation procedure. This procedure was performed in five batches to prevent intrabatch variability (due to the impossibility of carrying out some of its steps in parallel for all samples). This method was adapted from Kjaersgard et al.,[7] and its applicability for comparative purposes has recently been explored.[8] All protein extracts were then cleared from salts and contaminants using a standard TCA/acetone-based 2DE protein precipitation kit (Ready-Prep 2-D Cleanup Kit, Bio-Rad) and quantified using a standard Bradford colorimetric method.

Two-Dimensional Gel Electrophoresis (IPG-IEF/SDS-PAGE). Six hundred micrograms of protein from each sarcoplasmic extract was loaded onto 24 cm IPG ReadyStrip pH 4−7 strips (Bio-Rad) by passively reswelling them overnight in 450 μL of total volume (using a standard IPG-IEF buffer for sample dilution, as appropriate). Proteins were separated in the first dimension by isoelectric focusing using an Ettan IPGphor (Amersham), at 20 °C, for a total of about 43 kV·h. Strips were then equilibrated using standard Bio-Rad reduction/alkylation buffers (15 min each step), loaded onto manually cast large-format 12.5% Tris-HCl SDS-PAGE gels, and run at 50 mA/gel (after a short initial period at 10 mA/gel), using a standard Tris−glycine−SDS running buffer. After electrophoresis, gels were stained with EZBlue colloidal CBB stain (Sigma) according to the manufacturer's instructions. Due to the impossibility of running the whole 2DE procedure in parallel for all samples, three batches of IEF and five batches of SDS-PAGE were performed. Sample distribution among batches was chosen to prevent variable confounding by balancing and randomization (avoiding the introduction of any artificial correlation between sample source, preslaughter stress level, time of sampling, extraction/fractionation batch, IEF batch, and SDS-PAGE batch).

Gel Scanning and Image Analysis. After staining, each of the 30 gels was digitized using a GS-800 calibrated densitometer (Bio-Rad) at a 42.3 μm/pixel resolution and analyzed using Progenesis SameSpots 2DE gel analysis software (Nonlinear Dynamics, Newcastle upon Tyne, UK), which performs semiautomatic detection, alignment, background subtraction, and quantification of protein spots. The software automatically assigns a unique numeric identifier to each spot. Normalization of background-subtracted spot volumes across gels is done by estimating a per-gel gain factor calculated from a recursive median of the log-transformed spot abundance values, which makes it robust to spot volume distributions with abnormal skewness and/or kurtosis. As an alternative to SameSpots' native normalization algorithm, we also employed the variance stabilization and normalization (VSN) method, which applies an inverse hyperbolic sine transformation after removal of additive and multiplicative biases estimated with least trimmed sum of squares (LTS) regression.

Experimental spot p*I* values were estimated from the spots' horizontal positions on the 2DE gel, by linearly interpolating between the two pH extremes (4 and 7). Molecular weights were estimated by running a separate gel with an appropriate molecular weight marker to obtain a calibration curve for the estimation of a spot's $\log(M_w)$ based on its vertical position.

Data Visualization and Feature Selection. Data sets exported from SameSpots were then analyzed using the R statistical computing environment (The R Foundation for Statistical Computing, Vienna, Austria). Data visualization was performed using principal component analysis (PCA) and metric multidimensional scaling (MDS) taking $1 - |\tau|$ as dissimilarity measure, where τ is Kendall's rank correlation between gels. For variable selection, partial least-squares regression (PLS2) was used, as implemented in The Unscrambler software (Camo Software, Oslo, Norway). Forty-four distinct PLS models were obtained by choosing different normalization methods (both SameSpots' native algorithm and the VSN method); optional prefiltering of probably irrelevant spots (using the Mann−Whitney univariate test for comparison between groups, and taking a p value >0.05 threshold as indicative of low relevancy); choosing different scaling methods (autoscaling, group scaling, and mean-centering by subject followed by group scaling); and using three different *Y* matrices (where the *time* factor is expressed in three different ways). These models were obtained by progressive removal of features using jack-knife validation, in a way that the explained validated *Y*-variance and the validated correlation between PLS components and *Y*-matrix variables were maximized. The values obtained for these parameters were generally around 70−80% and 0.7−0.9, respectively. Protein spots that contributed to explain the *X*-matrix variation according to the *Y*-matrix factors (*treatment* and *time*) in more than 10 PLS models were considered for manual excision from the 2DE gels and subsequent identification by MS.

Protein Identification by MALDI-TOF-TOF. After reduction and alkylation (using DTT and iodoacetamide, respectively), protein spots were digested with trypsin and the reaction was stopped with 0.1% trifluoroacetic acid. After a concentration/desalting step, the peptides were cocrystallized with the matrix (DHB) on a MALDI plate and analyzed with an Ultraflex II MALDI-TOF-TOF mass spectrometer (Bruker-Daltonics). Spectra were obtained in positive reflector mode and externally calibrated using a tryptic digest of β-lactoglobulin. These were analyzed and converted to MS and MS/MS peak lists using FlexAnalysis 3.0 (Bruker-Daltonics), removing peaks known to be common MS contaminants (human keratin and trypsin autolysis products). The obtained peak lists were then used as input to MASCOT MS/MS Ion searches of the Actinopterygii subset of the NCBInr database, using the Matrix Science webserver (http://www.matrixscience.com/). These searches were performed by assuming the formation of single-charged peptides, carbamidomethylation of cysteine residues, possible oxidation of methionine residues, and up to one missed cleavage. Mass tolerance was 70 ppm for MS data and 0.5 Da for MS/MS data. A protein spot was considered to be reliably identified when at least one MS/MS spectrum could be associated with a specific peptide in the database with high certainty (E value < 0.05). Whenever no significant hits were obtained with the NCBInr database, searches were repeated against the Actinopterygii subset of the Vertebrates_EST database. The identity of nonannotated transcripts was assessed using blastp (http://blast.ncbi.nlm.nih.gov/) against the NCBInr database. For each identified spot, we also attempted to determine the specific isoform (whenever isoform-specific peptides could be identified from the MS/MS data).

RESULTS

Analysis of the 30 gel images enabled the detection and quantification of 313 spots across all gels. A representative example can be seen in Figure 1. Preliminary visualization of

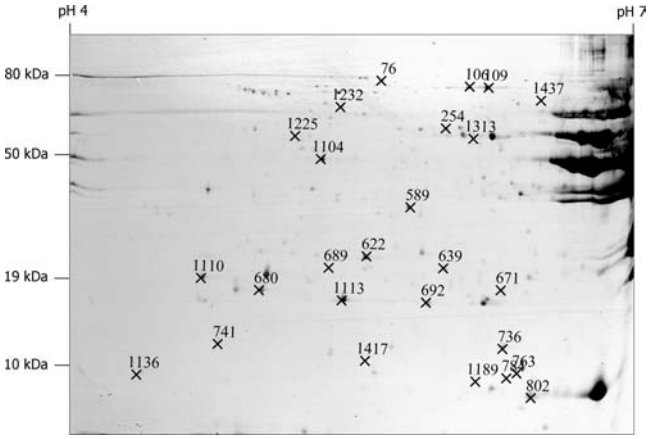

Figure 1. Representative high-resolution and contrast-enhanced example of obtained 2DE gels, denoting the position of reliably identified protein spots.

the 30 × 313 matrix using PCA (Figure 2) suggests the samples can be roughly divided into three clusters: prerigor unstressed fish (*cluster 1*); prerigor stressed fish (*cluster 2*); and postrigor stressed and unstressed fish (*cluster 3*). This implies the observed differences between treatments are greater prerigor than postrigor. Also, cluster 3 seems to be more similar to cluster 2 than to cluster 1, which suggests that, in general, the application of preslaughter stress seems to have sped the transition between the prerigor proteomic profile and the postrigor proteomic profile. This is consistent with our observations of both a quicker onset of rigor in fish subjected to preslaughter stress and a general reduction in the differences between the unstressed and stressed fish groups over time for other parameters (such as measured muscle pH).[6]

As can be seen in Figure I of the Supporting Information, most protein spots were not included in any of the 44 obtained PLS models, with only 79 of the 313 being included in more than 10 models. Visualization with PCA suggests this reduced 79-spot data set contains a lower amount of irrelevant information while simultaneously preserving most of the biological information (see Figure 2). Particularly interesting is the fact that true dimensionality of the data set is only clear in this second PCA, where the first two components can be directly associated with the two experimentally implied factors ("harvesting stress condition" and "time elapsed since slaughter").

These observations were confirmed by using a different similarity metric (based on Kendall's correlation) and using metric multidimensional scaling to plot the results in 2D (Supporting Information, Figure II).

Another interesting observation when several measured physiological parameters were compared with the results obtained by the proteomic analysis was that two of the protein spots showed a significant degree of correlation with the measured muscle pH (ρ = 0.80 and 0.89, respectively; or τ = 0.74 and 0.82, respectively, if Kendall's correlation measure is used), as can be seen in Figure IV of the Supporting Information. Repeated simulations with randomly permuted versions of the original data set seem to indicate that values of τ above 0.46 (or below −0.46) occur only by chance with a probability below 0.0001. Besides protein spots selected by PLS regression, we also sought to identify these two protein spots displaying correlation to measured muscle pH.

All nonoverlapping spots deemed relevant that displayed acceptable resolution and intensity were excised from the gels, digested with trypsin and subjected to MS analysis. Of these, we were able to reliably identify 25 of them (see Figure 1 and Table 1). It should be noted that, for some of the identified spots, observed deviations between estimated and theoretical molecular weights suggest that they are very likely to constitute proteolytic fragments of the respective full-length proteins. A quick overview of the results for these spots can be seen in Table 2 and the heatmap of Figure 3. More detailed time-dependent protein abundance profiles for these proteins can also be seen in Figure VI of the Supporting Information.

DISCUSSION

During the course of this study, we were able to observe time-variable post-mortem changes in the sarcoplasmic proteome of gilthead seabream modulated by preslaughter stress. Identified proteins included cytoskeletal proteins as well as proteins related to the redox homeostasis, proteasome/ubiquitin pathway, detoxification, energy homeostasis, and signal transduction. We sought to interpret observed changes in light of current literature. A schematic overview of the possible relationships between preslaughter stress and these cellular processes can be seen in Figure 4.

Energy Homeostasis and Signal Transduction. Efficient coupling of spatially segregated ATP-producing and ATP-consuming cellular processes requires the action of several enzymes belonging to the so-called "phosphotransfer networks", such as creatine kinase (CK), adenylate kinase (AK), nucleoside diphosphate kinase (NDPK), carbonic anhydrase (CA), and some glycolytic enzymes, which help to rapidly dissipate ATP/ADP gradients across the cell, effectively facilitating the spatial transmission of high-energy phosphoryl groups from ATP-producing to ATP-consuming sites. The high rate of energy production and consumption in active muscle suggests that phosphotransfer networks should have an essential role in the correct and efficient function of this tissue. This was evident from the 2DE gels of the sarcoplasmic fraction of muscle, where a high abundance of these proteins was observed (particularly CK).

During this study, a progressive increase in the abundance of an AK spot was noted in fish subjected to stress, although some of these seemed to have lower inductions (displaying an abundance temporal profile similar to control fish). On the other hand, given this spot's observed molecular weight, it is possible that it constitutes an ∼18 kDa proteolytic fragment of the 21 kDa full-length AK, which would imply a higher (but variable) degree of proteolysis in stressed fish, with nonstressed fish displaying a general lack of proteolytic activity toward AK. A possible explanation for the increase in proteolytic activity against AK might be that stress-induced expression of AK has simply increased availability of this protein, increasing the chances of proteolytic events involving AK. Another possibility is that changes in the ATP/ADP/AMP proportions due to induced preslaughter stress might affect steady-state concentrations of the different AK conformers, leading to a differential observed proteolytic activity toward AK depending on the pre-mortem energetic status. Finally, it also has to be considered

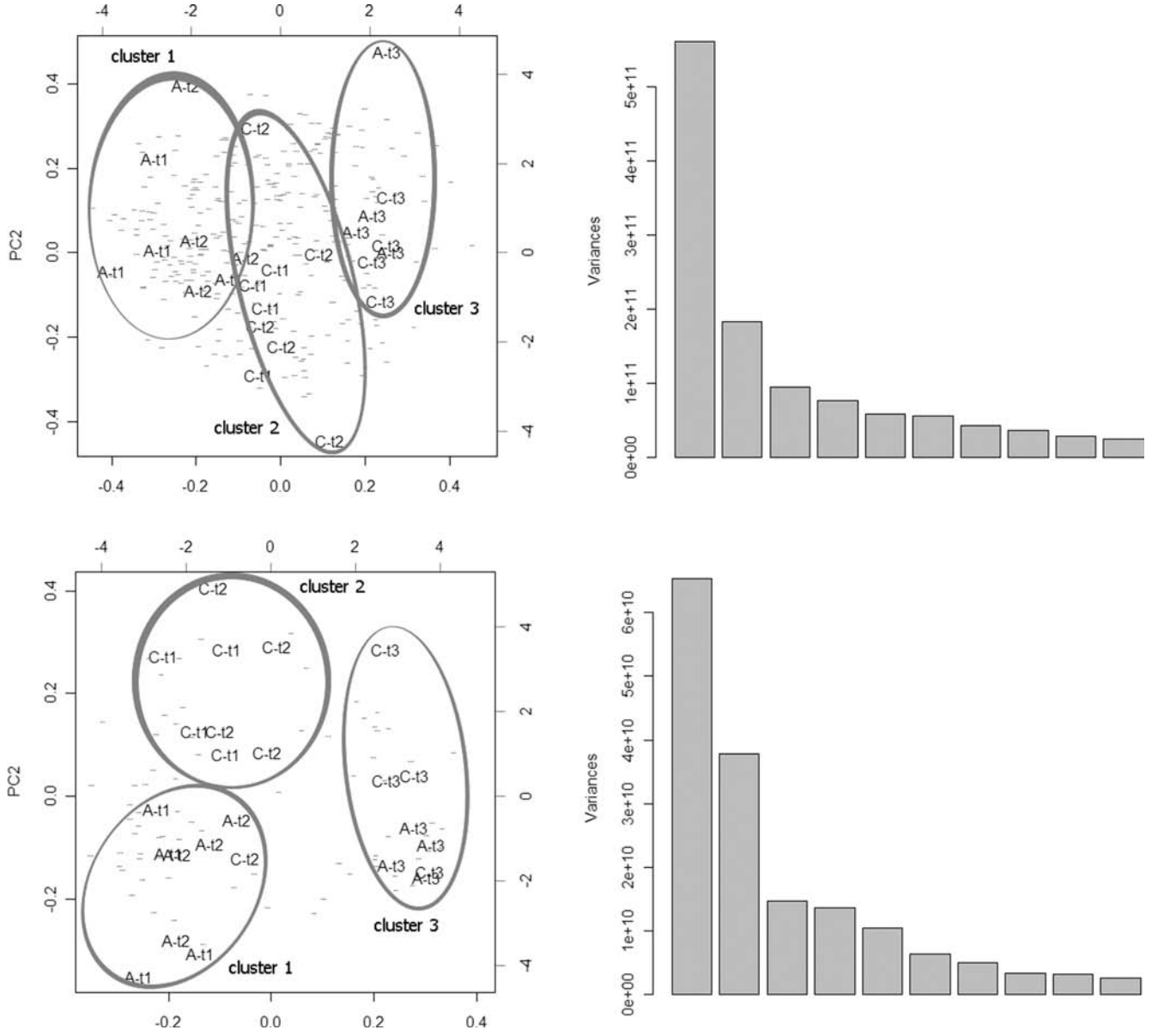

Figure 2. Principal component analysis before (above, 313 variables) and after variable selection (below, 79 variables). On the left are biplots showing the similarities between all samples (as measured by the Euclidian distance, after mean-centering and autoscaling). Samples are labeled "A" (for anesthesia) or "C" (for crowded) and the corresponding sampling time ("t1", "t2", or "t3", meaning t = 0, 6, and 48 h, respectively). The small horizontal gray lines represent variables (i.e., proteins spots). On the right is illustrated explained variance for each principal component.

that preslaughter stress might have simply sped the cascade of proteolysis (i.e., proteolytic activation of proteases), resulting in generally higher levels of proteolysis toward all sarcoplasmic proteins.

Besides AK, we were also able to detect three other protein spots (two NDPK spots and one CA spot), which are almost certainly proteolytic fragments. In both cases, stressed fish displayed increased abundance of these spots, compared to control (in the case of CA, at all sampling times; in the case of NDPK, only on later sampling time points). Also, a general trend of increased abundance over time could be observed for all spots. Explanations for the observed increase in the abundance of proteolytic fragments can be linked, as said above for AK, to several factors. At least in the particular case of NDPK, nucleotide binding has been shown to stabilize it,[9] suggesting that stress-induced ATP depletion might directly affect NDPK's susceptibility to proteolysis. Interestingly, recent studies on sea bass showed that NDPK muscle abundance is likely to decrease post-mortem, regardless of the fish storage temperature, due to proteolysis,[10,11] which is consistent with what we observed.

Another relevant protein was identified as phosphatidylethanolamine binding protein (PEBP), which is also known as the Raf-1 kinase inhibitor protein (RKIP), an ubiquitous protein with a role in signal transduction [namely, as a suppressor of the mitogen-activated protein kinase (MAPK) pathway].[12] Studies have shown RKIP prevents phosphorylation of MEK1/MAP2K1, NIK/MAP3K14, and TAK1/MAP3K7 through competitive inhibition, therefore suppressing signaling to downstream kinases and associated transcription factors (such as AP-1 and NF-κB).[13] In our experiment, increased levels of an RKIP proteolytic fragment in fish subjected to preslaughter stress were generally observed, as well as a positive correlation between elapsed time since slaughter and protein abundance in

Table 1. Reliably Sequenced Proteins, along with Relevant MS-Related Information[a]

spot ID	protein identification	accession no.	species	exptl M_w/pI	theorM_w/pI	coverage (%)	no. of peptide matches	best peptide match: sequence, E value	combined Mowse score
76	myosin binding protein C or H	AAI46704.1	*Danio rerio*	81 kDa/5.4	58 kDa/5.4	4	3	TGDWFTVLEHYHR, 9.2e−07	139
106	transferrin	CAL92187.1	*Chaenocephalus aceratus*	76 kDa/5.8	76 kDa/6.4	2	1	ASAEEQYYGYAGAFR, 0.00026	75
109	transferrin (inferred)			76 kDa/5.9					
254	antiquitin/ALDH7A1	AAX54912.1	*Acanthopagrus schlegelii*	57 kDa/5.7	56 kDa/5.9	7	5	AISFVGSNSAGEYIYER, 4.7e−09	231
589	*S*-formylglutathione hydrolase	ACO09141.1	*Osmerus mordax*	32 kDa/5.5	32 kDa/6.0	2	1	KIPVVFR, 0.0039	47
622	carbonic anhydrase**	AAQ89896.1	*Oreochromis mossambicus*	23 kDa/5.4	29 kDa/7.7	5	1	YPAELHLVHWNTK, 5.6e−07	104
639	glutathione *S*-transferase**	AAQ56182.1	*Sparus aurata*	21 kDa/5.7	35 kDa/8.5	22	5	LIPDSPAEQALTYQR, 3.5e−06	427
671	adenylate kinase 1-2*	ACM41863.1	*Epinephelus coioides*	18 kDa/5.9	21 kDa/7.6	31	6	KVDSELPVDEVFGQVSK, 1.8e−08	388
680	lactoylglutathione lyase*	ACO09023.1	*Osmerus mordax*	17 kDa/4.9	20 kDa/5.2	12	4	GFGHIGIAVPDVYEACK, 6.2e−07	143
689	proteasome α 2 subunit*	ACI66157.1	*Salmo salar*	21 kDa/5.2	26 kDa/6.0	8	1	LVQIEYALAAVAAGAPSVGIK, 7e−08	104
692	dj-1 protein*	CAG07041.1	*Tetraodon nigroviridis*	16 kDa/5.6	20 kDa/6.1	24	3	AGIAVTVAGLTGKEPVQCSR, 6.4e−10	204
736	cofilin 2 (muscle)**	NP_991263.1	*Danio rerio*	12 kDa/6.0	19 kDa/7.6	18	2	KEDLVFIFWAPEGAPLK, 4e−08	223
741	myosin light chain 2**	BAA95125.1	*Thunnus thynnus*	12 kDa/4.7	19 kDa/4.7	64	8	EFLEELLTTQCDR, 2.1e−07	705
763	nucleoside diphosphate kinase B**	AAG13336.1	*Gillichthys mirabilis*	10 kDa/6.0	17 kDa/6.8	19	2	TFIAVKPDGVQR, 0.0066	133
784	Cu/Zn superoxide dismutase	CAI79044.1	*Sparus aurata*	9 kDa/5.9	7 kDa/5.4	28	1	MLTLSGPLSIIGR, 7.1e−07	138
802	nucleoside diphosphate kinase B**	ADG29125.1	*Epinephelus coioides*	9 kDa/6.1	17 kDa/6.8	40	4	GDLCINIGR, 0.0023	159
1104	α-actin	AAA29847.1	*Styela clava*	45 kDa/5.1	42 kDa/5.2	20	6	SYELPDGQVITIGNER, 1.3e−07	486
1110	myosin light chain	BAA12731.1	*Cyprinus carpio*	19 kDa/4.6	21 kDa/4.7	13	3	VAYNQIADIMR, 4.7e−06	128
1113	phosphatidylethanolamine binding protein**	AAB06983.1	*Mus musculus*	16 kDa/5.2	21 kDa/5.2	18	2	YNLGAPVAGTCYQAEWDDYVPK, 2.5e−06	172
1136	β-actin**	AAH45846.1	*Danio rerio*	9 kDa/4.3	42 kDa/5.3	2	1	IWHHTFYNELR, 9.6e−05	80
1189	ubiquitin-conjugating enzyme E2 variant 2**	NP_998680.1	*Danio rerio*	9 kDa/5.9	16 kDa/7.8	8	2	VECGSRYPEAAPTVR, 0.0085	93
1225	26S protease regulatory subunit 6B	AAH55215.1	*Danio rerio*	52 kDa/5.0	47 kDa/5.0	15	4	ENAPAIIFIDEIDAIATK, 0.00013	303
1232	glycogen phosphorylase**	AJ719440.1	*Gallus gallus*	65 kDa/5.2	97 kDa/6.0	1	1	IIDGWQVEEADDWLR, 2.6e−05	86
1313	26S protease regulatory subunit 6A	AAB24840.1	*Homo sapiens*	53 kDa/5.8	49 kDa/5.1	12	4	DSYLILETLPTEYDSR, 5.4e−08	322
1417	peroxiredoxin 5**	ADI78068.1	*Sparus aurata*	11 kDa/5.3	28 kDa/8.9	7	1	AVDLLLDSDQIVQVLGNKR, 4.7e−10	129
1437	skeletal α-actin	CAA24598.1	*Sparus aurata*	71 kDa/6.1	42 kDa/5.5	7	2	SYELPDGQVITIGNER, 4.8e−08	168

[a]Theoretical M_w and pI values were estimated from the protein's composition (based on available sequence data). Only peptides with E value below 0.05 (discarding oxidized versions and other duplicates) were counted for the calculation of the number of matched peptides per protein, estimated coverage, and combined Mowse score. Entries marked with an asterisk (*) indicate a possibility that the identified spot constitutes a proteolytic fragment, whereas entries with a double asterisk (**) indicate that it is very likely that the identified spot constitutes a proteolytic fragment.

dx.doi.org/10.1021/jf301766e | J. Agric. Food Chem. 2012, 60, 9443−9453

Table 2. Differential Expression Trends and Univariate Statistics for Each Identified Protein[a]

		harvesting stress effect anesthesia → crowding			time effect					
					T0 → T6		T0 → T48		T6 →T48	
spot	protein identification	T0	T6	T48	A	C	A	C	A	C
76	myosin binding protein C or H	**2.62***	**2.84***	−0.42	0.16	**1.87**	**1.87**	−0.24	−0.27	−0.45
106	transferrin	0.93	**2.07***	0.89	−0.36	0.77	0.25	−0.12	0.58	0.53
109	transferrin (inferred)	0.28	**2.63***	**1.12**	−0.72	**1.26***	0.29	0.72	0.69	**1.01**
254	antiquitin/ALDH7A1	0.34	**−1.28***	**−1.03**	0.88	0.13	**1.31***	−0.92	0.76	0.03
589	*S*-formylglutathione hydrolase	0.33	**1.93***	0.54	−0.32	**1.33***	**1.09***	**1.38***	0.89	**1.03***
622	carbonic anhydrase**	**1.42***	**1.02**	0.77	0.33	**2.21***	**3.11***	0.20	0.78	0.85*
639	glutathione *S*-transferase**	**1.97***	**1.73***	**1.15***	0.31	0.16	0.40	0.10	0.74	0.77
671	adenylate kinase 1−2*	**2.31***	**1.51**	**1.42***	−0.25	0.66	0.38	0.73	0.63	**1.11**
680	lactoylglutathione lyase*	0.83	−0.55	**1.47***	**1.53***	0.30	**3.38***	−0.26	**2.17***	0.93
689	proteasome α 2 subunit*	0.56	0.59	0.50	0.24	**2.06***	**2.00***	0.11	0.74	0.76
692	dj-1 protein*	**1.28**	**2.88***	0.75	0.84	**6.01***	**5.09***	**2.35***	0.98*	**1.21***
736	cofilin 2 (muscle)**	−0.02	**1.86***	0.68	−0.60	**5.12***	**6.27***	**1.35***	0.88*	0.99*
741	myosin light chain 2**	**−1.55***	−0.86	0.27	**1.88***	**−3.02***	−0.93	**1.06**	−0.35	0.56
763	nucleoside diphosphate kinase B**	−0.10	**1.54***	0.95	**−2.22***	0.45	**−2.01***	**−1.23***	0.74	0.43
784	Cu/Zn superoxide dismutase	−0.20	0.84	0.64	−0.95	**2.64***	**1.43***	0.02	0.98	0.98*
802	nucleoside diphosphate kinase B**	−0.86	**1.50***	**1.18***	**−3.13***	−0.78	**−4.07***	−0.34	0.61	0.52
1104	α-actin	**−1.49***	**−1.55**	−0.03	−0.79	**−2.63***	**−1.88***	−0.22	−0.78	**−1.40***
1110	myosin light chain	**−1.31***	−0.63	0.67	0.89	−0.52	**1.27**	**1.42***	0.76	**1.37***
1113	phosphatidylethanolamine binding protein**	**1.70***	0.86	0.82	0.71	**2.22***	**2.39***	0.17	**1.04***	**1.10***
1136	β-actin**	**−1.75***	−0.82	−0.86	0.59	**−1.88**	**−1.63***	0.51	−0.91	−0.53
1189	ubiquitin-conjugating enzyme E2 variant 2**	−0.01	−0.18	**1.45***	0.99	**1.49**	**2.67***	**1.24**	**2.27***	**2.78***
1225	26S protease regulatory subunit 6B	**1.73***	**−1.23**	−0.03	**1.54***	**−8.93***	**−4.50***	**−1.36**	**−2.41***	**−4.50***
1232	glycogen phosphorylase**	0.67	**2.00***	0.73	−0.76	**1.18**	0.32	0.99	−0.05	0.61
1313	26S protease regulatory subunit 6A	0.41	**−1.57***	**−1.06**	−0.66	−0.67	**−1.07**	−0.77	−0.15	−0.78
1417	peroxiredoxin 5**	−0.66	**−1.33***	−0.23	0.12	**−2.72***	**−1.97***	−0.48	−0.83	**−1.55***

[a]Direction and magnitude of effect size (Cohen's *d*) for the stress factor (at each time point) and for the time factor (separately for anesthesia and crowded groups). Effect sizes >1 standard deviation are marked in bold. An asterisk (*) next to a number denotes statistical significance of the observed effect (assessed by Mann−Whitney−Wilcoxon's *U* test, $p < 0.05$). Protein names marked with an asterisk (*) indicate a possibility that the identified spot constitutes a proteolytic fragment, whereas entries with a double asterisk (**) indicate that it is very likely that the identified spot constitutes a proteolytic fragment.

both treatments. It is possible that the phosphorylation state of RKIP might affect its susceptibility to proteasome-mediated proteolysis,[14] which could be the underlying link relating preslaughter stress with increased RKIP proteolysis.

Another protein associated with energy homeostasis in muscle is glycogen phosphorylase, which is responsible for mobilization of glucose stored as glycogen, enabling a quick response to increased energy requirements. In this study, we observed a higher abundance of a proteolytic fragment of glycogen phosphorylase in fish subjected to preslaughter stress, especially at 6 h after slaughter, although the effect is still visible 48 h after slaughter. This difference, again, points toward higher levels of proteolysis in fish stressed preslaughter, possibly associated with a higher degree of myofibrilar degeneration (as glycogen phosphorylase is known to tightly bind to myofibrillar proteins, which suggests its apparent abundance in sarcoplasmic extracts is likely to be affected by leakage and oxidation of myofibrillar proteins[15]).

Cellular Response to Redox Stress. Peroxiredoxin 5 is a 3-Cys hypoxia-inducible mitochondrial isoform of peroxiredoxin in which, when overexpressed, seems to induce a protective effect against oxidative stress-induced apoptosis. During our experiment, the post-mortem abundance of a proteolytic fragment of this protein is progressively reduced with time. This would imply that peroxiredoxin 5 is particularly susceptible to early proteolysis, as high amounts of this fragment can be seen on the first sampling, with subsequent samplings showing a clear reduction in the abundance of this spot. Again, preslaughter stress appears to hasten this process, as stressed fish displayed consistently lower abundance levels of this proteolytic fragment at all time points, compared to unstressed fish.

Another important element in cellular redox homeostasis is the Cu/Zn superoxide dismutase, a protein that catalyzes the conversion of superoxide radicals into oxygen and hydrogen peroxide. Although no significant differences were found in stressed fish, the abundance of this protein was increased postrigor in both treatments (compared to prerigor), suggesting an increased expression (or limited turnover) of this protein. This could be a reflection of the importance of this protein in the cellular defense against the highly toxic superoxide radicals, in contrast with peroxiredoxin 5, which can be functionally complemented by the activity of other peroxidases (such as catalase).

Iron is a metabolically essential metal that can act as a pro-oxidant when in its free form, catalyzing the formation of hydroxyl and peroxide radicals from hydrogen peroxide. The pro-oxidant activity of iron in skeletal muscle is mainly controlled by transferrin and ferritin, which have the capacity to chelate this metal, maintaining it in the ferric form (Fe^{3+}). Two spots identified as transferrin displayed generally higher abundance in fish subjected to preslaughter stress, especially at

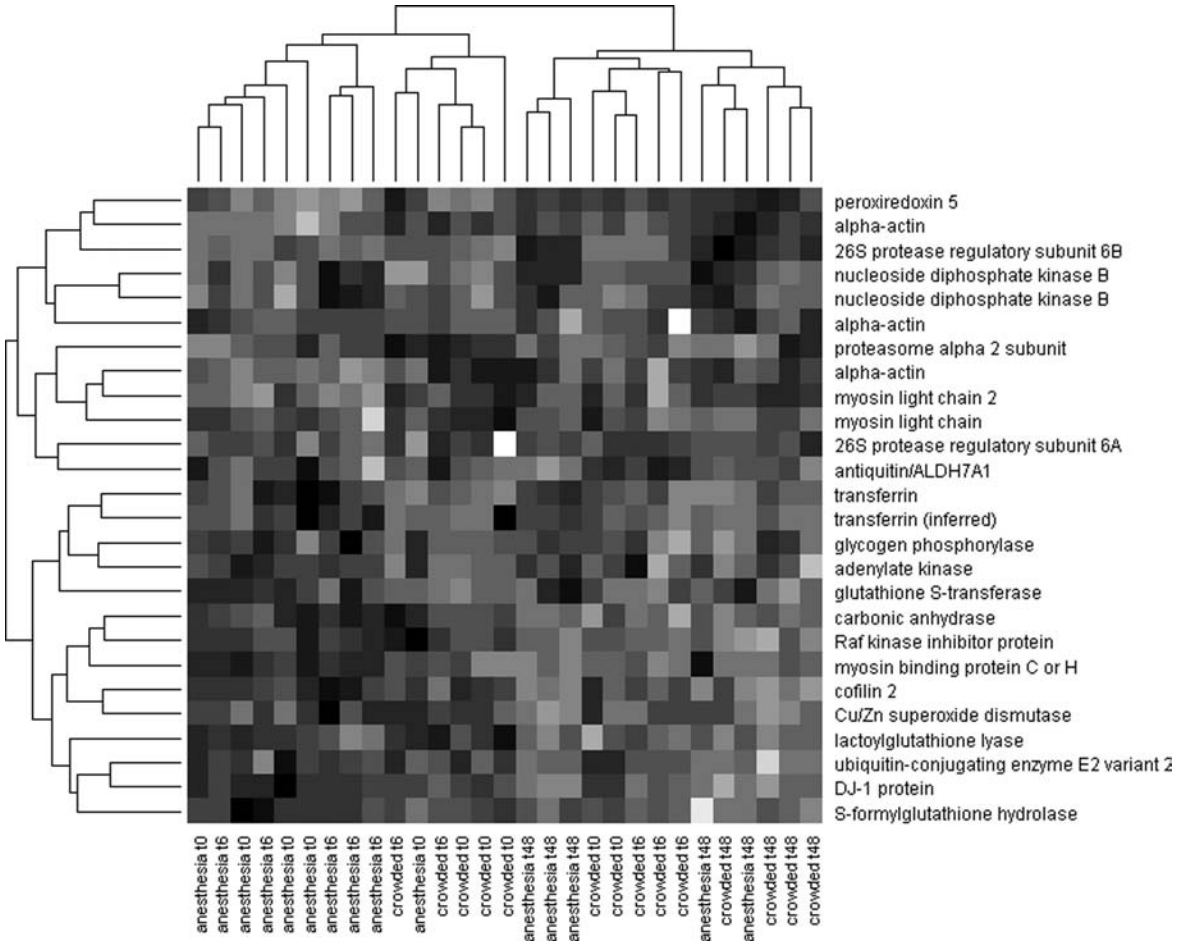

Figure 3. Heatmap showing relative abundance of each sequenced spot across all samples, along with simultaneous clustering of spots and gels (using Euclidian distance as dissimilarity measure and the "complete linkage" criterion for agglomerative hierarchical clustering) using this reduced data set. Dark colors indicate lower than average expression, whereas light colors indicate higher than average expression.

6 and 48 h after slaughtering. This could be a sign of a higher degree of iron import into muscle (complexed with transferrin) or a lower degree of transferrin recycling in response to the applied stress. It is interesting to note that higher levels of transferrin have already been detected in the sarcoplasmic fraction of PSE (pale, soft, exudative) bovine meat,[16] having been explained as a possible consequence of the effects of hypoxia on angiogenesis and tissue remodeling. Further insight into the interaction between preslaughter stress and iron homeostasis in muscle could be obtained if the levels of ferritin and total iron were also assessed in parallel.

Another protein related to cellular redox stress is the DJ-1 protein (also known as PARK7, due to its association with Parkinson's disease). The biological function of this protein is still not completely figured out, although it seems to have (among others) antioxidant and protein chaperone roles and, specifically in the skeletal muscle of mice, to be involved in the regulation of the Ca^{2+} pool.[17] During the course of our study, we observed an increase over time in the abundance of what appears to be a proteolytic fragment of this protein, as well as generally higher abundance in fish subjected to preslaughter stress. At least two experiments on post-mortem muscle degradation in land animals also revealed an increase in the abundance of several DJ-1 protein spots over time.[18,19] Besides that, another study on the effects of preslaughter stress on the soluble muscle proteome of trout showed results consistent with ours: the application of preslaughter stress induced lower concentrations of the full-length protein in muscle, pointing toward a higher degree of proteolytic activity.[20]

Detoxification Processes. Antiquitin (also known as ALDH7A1) is a highly conserved member of the aldehyde dehydrogenase family that catalyzes conversion of L-2-amino-adipate-6-semialdehyde (an intermediate in lysine catabolism) into L-2-aminoadipate, using NAD^+ as cofactor. A recent study with purified recombinant human ALDH7A1 suggests it is probably also related to osmotic regulation (due to observed betaine aldehyde dehydrogenase activity) and lipid peroxidation (due to observed dehydrogenase activity regarding some lipid peroxidation products).[21] During our experiment, slightly decreased levels of ALDH7A1 were detected in fish subjected to preslaughter stress, specifically after 6 h post-mortem. This could be a sign of increased oxidation, proteolysis, and/or aggregation of ALDH7A1 in fish subjected to preslaughter stress.

S-Formylglutathione hydrolase (also known as esterase D) participates in formaldehyde detoxification by catalyzing the hydrolysis of *S*-formylglutathione into formate and glutathione. Formaldehyde can be endogenously produced from methanol and methylamine, being also a side product of methionine catabolism, histidine catabolism, and oxidative demethylation of nucleic acids. During our experiment, we observed generally increased levels of *S*-formylglutathione hydrolase in fish

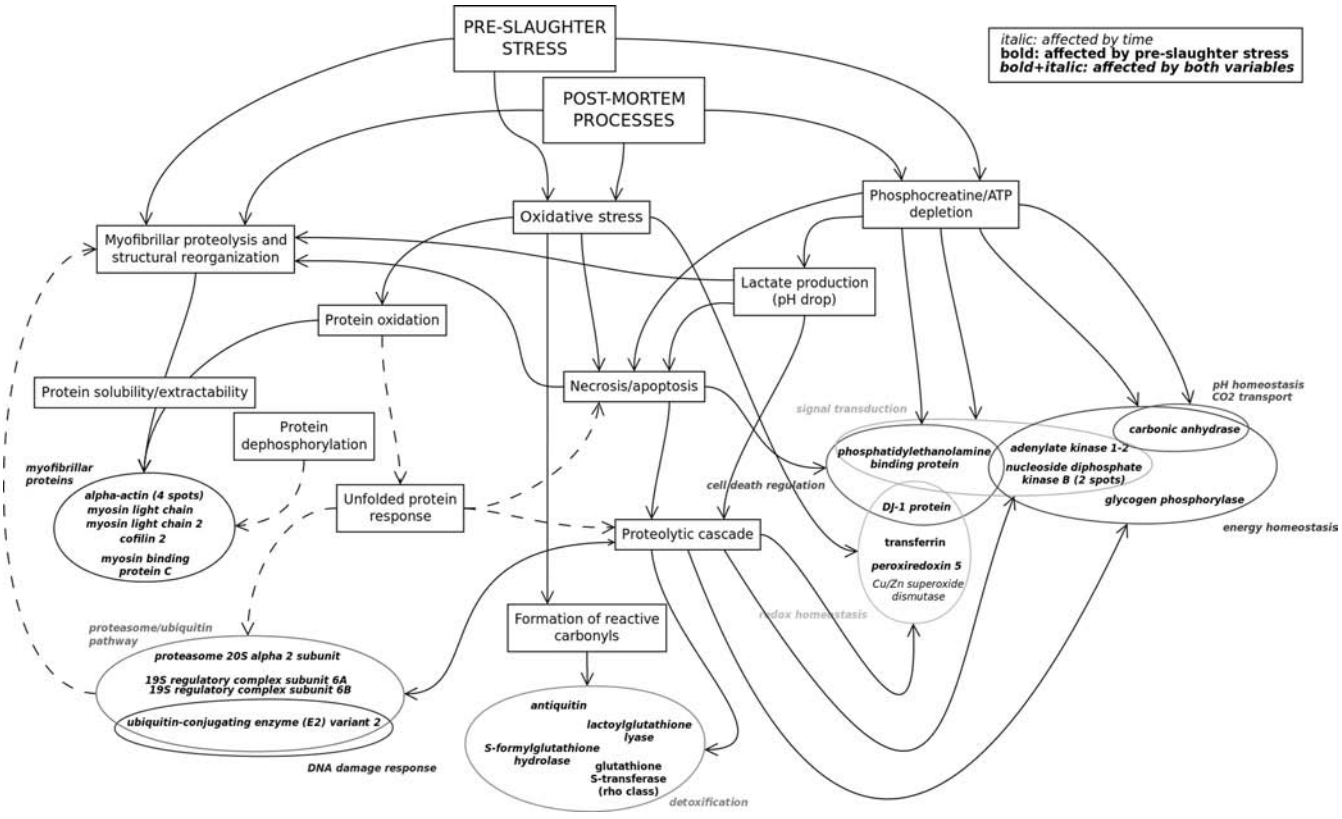

Figure 4. Schematic overview of the putative interactions between induced preslaughter stress and known post-mortem processes in muscle. Broken lines indicate not directly observed or assessed relation, while full lines denotes either observed or highly likely relations and events.

subjected to preslaughter stress at early time points, which suggests a direct cellular response to induced physiological stress. We also observed a small induction of this protein (regardless of stress state) after slaughter, which is consistent with observations on post-mortem porcine muscle.[22]

Furthermore, there were two other spots identified as proteolytic fragments of proteins also involved in glutathione metabolism: glutathione *S*-transferase and lactoylglutathione lyase. In the case of glutathione *S*-transferase, it is interesting to note that nonstressed fish display very stable low abundances for this proteolytic fragment, whereas stressed fish display relatively higher and more variable abundances. In the case of lactoylglutathione lyase, abundance increases over time, but preslaughter-stressed fish display generally higher abundance levels. This seems to indicate that the breakdown of the detoxification systems is generally hastened by the action of preslaughter stress.

One last fact to consider in the interpretation of observations related to the detoxification pathways is that both groups of fish were slaughtered using a lethal dosage of isoeugenol. As suggested by Matos et al.,[6] it is possible that isoeugenol might interact with oxidative stress and detoxification processes.

Proteasome/Ubiquitin Pathway. Although the caspase pathway seems to be the most important proteolytic system regarding fish muscle death and post-mortem degradation, there are signs that other proteolytic systems are likely to be involved (namely, the calpain, cathepsin, matrix metalloprotease, and proteasome systems) and that the relative importance of these systems on fish meat quality may be species-dependent. During our experiment, we observed abundance variations in several spots related to the 26S proteasome system: two of them are components of the 19S regulatory complex, one is a fragment of a component of the 20S proteasome, and the last one is a fragment of a ubiquitin-conjugating enzyme variant.

The abundance of two components (with ATPase activity) of the 19S regulatory complex, namely, the 6A subunit (also known as S6′, PSMC3, TBP1, or Rpt5) and the 6B subunit (also known as S6, PSMC4, TBP7, or Rpt3), was seen to change over time, depending on preslaughter stress levels. According to our observations, the abundance of the 6A subunit had a tendency to stabilize over time and there seemed to be lower amounts of this subunit in stressed fish. Because this subunit is involved in polyubiquitin recognition, this may imply either that the proteasome pathway has lower proteolytic activity in stressed fish or that it occurs via the ubiquitin-independent pathway (which acts preferentially during oxidative stress). Interestingly, the 6A subunit has been implicated in the regulation of HIF1α abundance (a transcription factor that regulates gene expression in response to hypoxia), mediated by its interaction with pVHL (an E3 enzyme). In fact, overexpression of the 6A subunit has been shown to promote HIF1α degradation, and blocking its expression via siRNA has been shown to reduce HIF1α degradation by the proteasome.[23] This suggests that decreased levels of this subunit could constitute a regulatory mechanism to increase HIF1α half-life in response to the applied preslaughter stress. In the case of subunit 6B, the time profile seems to suggest a post-mortem induction followed by a progressive reduction in abundance (i.e., a peak), which was delayed in control fish (compared to fish subjected to preslaughter stress). Still, given the low abundance of this protein at 48 h in both groups, the idea that the ubiquitin-independent pathway and/or other proteolytic pathways

contribute more significantly for post-mortem muscle degradation than the ubiquitin-dependent pathway seems plausible.

With regard to the proteolytic fragments observed, for the case of ubiquitin-conjugating enzyme E2 variant 2, an increase in the abundance of this fragment could be observed over time, with preslaughter stress inducing even higher levels. This effect is more pronounced at later time points, again suggesting a higher degree of proteolysis in preslaughter-stressed fish. In the case of the proteolytic fragment of 20S proteasome subunit α 2, it seems to increase over time for nonstressed fish, whereas, for stressed fish, it initially increases and then decreases in abundance, resulting in distinct abundance levels at 48 h (compared to nonstressed). This should be a sign of proteolytic activity in stressed fish against this fragment, suggesting again generally higher levels of proteolytic activity in preslaughter-stressed fish.

The results obtained therefore suggest either a shift from ubiquitin-dependent to ubiquitin-independent proteasome proteolytic activity or a general breakdown of the proteasome system, suggesting this system might be of secondary relevance regarding post-mortem proteolytic events in gilthead seabream muscle. It is nevertheless possible that some of the observed changes reflect the role of the proteasome in the post-translational regulation (i.e., turnover) of transcription factors.

Myofibrillar Proteins. After slaughtering, biochemical and physical changes that occur in fish muscle have a significant impact on the oxidation, solubility, phosphorylation, and proteolytic state of the structural/contractile proteins contained in the myofibrils. Analysis of the presence of these proteins in sarcoplasmic extracts has to also take into account the phenomenon of leakage that is associated with post-mortem myofibril degeneration.

In this work, we observed changes in the abundance of several putative myofibrillar proteins in our sarcoplasmic extracts: actin (three spots: apparently one full-length and two actin fragment spots), myosin light chain 1, myosin light chain 2, cofilin-2, and myosin binding protein (isoform C or H).

The three actin spots showed a general reduction in abundance over time. These could be a reflection of proteolytic activity toward actin and/or reduced protein solubility due to denaturation/aggregation. For two of those spots (the ones with lower molecular weight), the group subjected to preslaughter stress displayed lower abundance, whereas the other spot (apparently full-length actin) showed no significant differences between groups. This general reduction in actin abundance over time (for both full-length actin and fragments) can be explained by denaturation and aggregation due to post-mortem oxidative stress, which could reduce their extractability. If this assessment is correct, this seems to be an indirect confirmation of higher levels of oxidative stress in fish subjected to preslaughter stress.

The two myosin light chains identified during this experiment also displayed generally lower abundance in fish subjected to preslaughter stress. One of them (myosin light chain 1, a nonphosphorylatable isoform) appeared at a very high molecular weight, which suggests it could be some soluble aggregate or an otherwise covalently modified form of the protein. Its abundance apparently increased over time, but no significant differences between groups could be noted at 48 h post-mortem. The other myosin light chain spot observed (isoform 2, phosphorylatable) displayed an induction around 6 h post-mortem, and then its abundance levels fell again to low levels. If this specific spot corresponds to the phosphorylated isoform of this protein, the observed abundance profile could just be a reflection of the post-mortem myofibril contraction dynamics and energetic state.

Myosin binding protein (MyBP) is mainly localized in the C-zone of the thick filament, aiding in the assembly and maintenance of the myosin bundles that constitute the thick filaments. We have observed an ultimate high abundance of MyBP in both groups. In the group subjected to preslaughter stress, MyBP levels were already high immediately after slaughter, which suggests a contribution of preslaughter stress to hasten the process of post-mortem myofibril disassembly, increasing MyBP extractability.

Interestingly, previous observations by Jessen et al., correlating 2DE with sensory analysis data, suggest actin, fast myosin light chain 2, myosin binding protein, and phosphorylated cofilin-2 may have a relationship with rainbow trout muscle texture. Western blot with anti-phospho-cofilin confirmed positive correlation of phosphorylated cofilin-2 abundance measured immediately after slaughter with juicy texture, suggesting cofilin-2 dephosphorylation is an important mechanism influencing juiciness in rainbow trout fish muscle (unpublished results). A study on pig muscle identified a cofilin-2 spot in the TES-soluble fraction of the muscle, which displayed decreased abundance over time.[22] In our case, we have identified a cofilin-2 spot that displayed increased abundance over time, with a negligible preslaughter stress effect. This is consistent with the fact that no significant differences were noted in terms of instrumentally measured texture parameters between our control and stressed groups.[6]

In general, when observing this group of proteins as a whole, although transient effects can be seen immediately after slaughter and at 6 h after slaughter, no significant differences can be seen at 48 h between the control and stressed groups.

Correlations between Proteomic and Physiological/Biochemical Observations. During this study, we decided to comeasure several physiological and biochemical parameters on the same set of gilthead seabream muscle samples, in parallel with the proteomic analysis. Besides providing us with a more complete view of the interaction of preslaughter stress with the post-mortem cellular processes in the muscle tissue, it enabled us to look for correlations between proteomic and non-proteomic observations that could be useful in the discovery and validation of surrogate measurements for the estimation of proteomic data from (possibly higher throughput and cheaper to obtain) nonproteomic data.

As mentioned under Results, the only relatively strong correlations observed were between measured pH values (shown in Figure III of the Supporting Information) and the abundance levels of two protein spots (see Figure IV of the Supporting Information). So far, we could only identify one of the spots as being one of the α-actin spots, although the unidentified spot (referred to as "spot 1115") displays an even better correlation with measured muscle pH. It is interesting to note that none of these variables correlate well with elapsed time since slaughter, so it is unlikely that these observed correlations are a simple reflection of time, because the relationship remains even if we calculate the partial correlations (with the influence of the time variable removed).

With regard to the underlying reasons for the observed correlation between measured muscle pH and an α-actin spot, it might be difficult to pinpoint them without more information. Besides differences in protein abundance, the

observed change in spot abundance should be due to leakage of myofibrillar proteins, but may also involve post-translational modifications (e.g., oxidation state, phosphorylation) and/or changes in solubility/extractability.

Therefore, although any causal relationship between measured muscle pH and the abundance of such proteins, particularly myofibrillar ones, in the sarcoplasmic fraction of muscle should not be assumed without further data, it might be interesting to further explore this possibility, if any of these proteins are shown to be predictive of some specific physiological state of the muscle.

Final Considerations. Regardless of the fine details of how the physiological response to preslaughter stress occurs in the muscle of gilthead seabream, there are clear modulations of the post-mortem cellular processes, especially at the level of cytoskeletal/myofibrillar proteins, energy homeostasis processes, response to oxidative stress, signal transduction, and cell cycle regulation, with most of these changes being attributable to myofibril degeneration and oxidative and proteolytic activity. Although some of the specific proteins identified have not yet been characterized as being specifically associated with post-mortem processes in fish muscle, the overall results generally follow what is expected, given what is currently known about the cellular response to external sources of stress and energy depletion in muscle.

Despite the observed differences between the low-stress and high-stress groups (especially in the early time points) at the proteome level and in terms of measured muscle pH, there were no observable differences between groups in terms of texture properties (namely, hardness and cohesiveness of cooked and raw fillets).[6] This shows, on the one hand, a relative robustness of gilthead seabream muscle properties to preslaughter stress and, on the other hand, the sensitivity of proteomic data in detecting a biological response to certain stimulus, even when no differences are apparent according to macroscopic quality criteria. These factors emphasize the relevance of proteomics in the context of animal farming, not only in the field of fish welfare and harm reduction but also in fish quality, given the observed hastening effect of preslaughter stress on post-mortem muscle degradation processes.

■ ASSOCIATED CONTENT

Supporting Information

Additional figures. This material is available free of charge via the Internet at http://pubs.acs.org.

■ AUTHOR INFORMATION

Corresponding Author

*Postal address: Centro de Ciências do Mar do Algarve (CCMAR), Universidade do Algarve, Campus de Gambelas, 8005-139 Faro, Portugal. E-mail: tome@tomesilva.com.

Funding

This study was funded by Fundação para a Ciência e Tecnologia, project TEXBREAM (PTDC/MAR/70858/2006). T.S.S. was supported by FCT grant SFRH/BD/41392/2007. E.M. was supported by FCT grant SFRH/BD/40886/2007. All experimental procedures complied with the Guidelines of the European Union Council (86/609/EU) for the use of laboratory animals.

Notes

The authors declare no competing financial interest.

■ REFERENCES

(1) Ashley, P. J. Fish welfare: current issues in aquaculture. *Appl. Anim. Behav. Sci.* **2007**, *104*, 199−235.

(2) Ayala, M. D.; Abdel, I.; Santaella, M.; Martinez, C.; Periago, M. J.; Gil, F.; Blanco, A.; Albors, O. L. Muscle tissue structural changes and texture development in sea bream, *Sparus aurata* L., during post-mortem storage. *LWT−Food Sci. Technol.* **2010**, *43*, 465−475.

(3) Caballero, M. J.; Betancor, M.; Escrig, J. C.; Montero, D.; Monteros, A. E. D.; Castro, P.; Gines, R.; Izquierdo, M. Post mortem changes produced in the muscle of sea bream (*Sparus aurata*) during ice storage. *Aquaculture* **2009**, *291*, 210−216.

(4) Martinez, T. F.; Suarez, M. D.; Saez, M. I.; Alferez, B.; Garcia-Gallego, M. Changes in muscle properties during postmortem storage of farmed sea bream (*Sparus aurata*). *J. Food Process Eng.* **2011**, *34*, 922−946.

(5) Matos, E.; Silva, T. S.; Tiago, T.; Aureliano, M.; Dinis, M. T.; Dias, J. Effect of harvesting stress and storage conditions on protein degradation in fillets of farmed gilthead seabream (*Sparus aurata*): a differential scanning calorimetry study. *Food Chem.* **2011**, *126*, 270−276.

(6) Matos, E.; Goncalves, A.; Nunes, M. L.; Dinis, M. T.; Dias, J. Effect of harvesting stress and slaughter conditions on selected flesh quality criteria of gilthead seabream (*Sparus aurata*). *Aquaculture* **2010**, *305*, 66−72.

(7) Kjaersgard, I. V. H.; Jessen, F. Two-dimensional gel electrophoresis detection of protein oxidation in fresh and tainted rainbow trout muscle. *J. Agric. Food Chem.* **2004**, *52*, 7101−7107.

(8) Silva, T. S.; Cordeiro, O.; Jessen, F.; Dias, J.; Rodrigues, P. M. Reproducibility of a fractionation procedure for fish muscle proteomics. *Am. Biotechnol. Lab.* **2010**, *28*, 8−13.

(9) Souza, T. A. C. B.; Trindade, D. M.; Tonoli, C. C. C.; Santos, C. R.; Ward, R. J.; Arni, R. K.; Oliveira, A. H. C.; Murakami, M. T. Molecular adaptability of nucleoside diphosphate kinase b from trypanosomatid parasites: stability, oligomerization and structural determinants of nucleotide binding. *Mol. BioSyst.* **2011**, *7*, 2189−2195.

(10) Terova, G.; Addis, M. F.; Preziosa, E.; Pisanu, S.; Pagnozzi, D.; Biosa, G.; Gornati, R.; Bernardini, G.; Roggio, T.; Saroglia, M. Effects of postmortem storage temperature on sea bass (*Dicentrarchus labrax*) muscle protein degradation: analysis by 2-D DIGE and MS. *Proteomics* **2011**, *11*, 2901−2910.

(11) Addis, M. F.; Pisanu, S.; Preziosa, E.; Bernardini, G.; Pagnozzi, D.; Roggio, T.; Uzzau, S.; Saroglia, M.; Terova, G. 2D DIGE/MS to investigate the impact of slaughtering techniques on postmortem integrity of fish filet proteins. *J. Proteomics* **2012**, *75*, 3654−3664.

(12) Sedivy, J. M.; Yeung, K.; Janosch, P.; McFerran, B.; Rose, D. W.; Mischak, H.; Kolch, W. Mechanism of suppression of the Raf/MEK/extracellular signal-regulated kinase pathway by the Raf kinase inhibitor protein. *Mol. Cell. Biol.* **2000**, *20*, 3079−3085.

(13) Yeung, K. C.; Rose, D. W.; Dhillon, A. S.; Yaros, D.; Gustafsson, M.; Chatterjee, D.; McFerran, B.; Wyche, J.; Kolch, W.; Sedivy, J. M. Raf kinase inhibitor protein interacts with NF-κ B-inducing kinase and TAK1 and inhibits NF-κ 13 activation. *Mol. Cell. Biol.* **2001**, *21*, 7207−7217.

(14) Moen, E. L.; Wen, S.; Anwar, T.; Cross-Knorr, S.; Brilliant, K.; Birnbaum, F.; Rahaman, S.; Sedivy, J. M.; Moss, S. F.; Chatterjee, D. Regulation of RKIP function by *Helicobacter pylori* in gastric cancer. *PLoS ONE* **2012**, *7*, e37819.

(15) Chowrashi, P.; Mittal, B.; Sanger, J. M.; Sanger, J. W. Amorphin is phosphorylase; phosphorylase is an α-actinin-binding protein. *Cell Motil. Cytoskeleton* **2002**, *53*, 125−135.

(16) Laville, E.; Sayd, T.; Morzel, M.; Chambon, C.; Franck, M.; Figwer, P.; Larzul, C.; Le Roy, P.; Monin, G.; Cherel, P. Proteome analysis of the sarcoplasmic fraction of pig semimembranosus muscle: implications on meat color development. *J. Agric. Food Chem.* **2006**, *54*, 2732−2737.

(17) Shtifman, A.; Zhong, N.; Lopez, J. R.; Shen, J.; Xu, J. Altered Ca^{2+} homeostasis in the skeletal muscle of DJ-1 null mice. *Neurobiol. Aging* **2011**, *32*, 125−32.

(18) Hollung, K.; Jia, X. H.; Ekman, M.; Grove, H.; Faergestad, E. M.; Aass, L.; Hildrum, K. I. Proteome changes in bovine longissimus thoracis muscle during the early postmortem storage period. *J. Proteome Res.* **2007**, *6*, 2720−2731.
(19) Laville, E.; Sayd, T.; Morzel, M.; Blinet, S.; Chambon, C.; Lepetit, J.; Renand, G.; Hocquette, J. F. Proteome changes during meat aging in tough and tender beef suggest the importance of apoptosis and protein solubility for beef aging and tenderization. *J. Agric. Food Chem.* **2009**, *57*, 10755−10764.
(20) Morzel, M.; Chambon, C.; Lefevre, F.; Paboeuf, G.; Laville, E. Modifications of trout (*Oncorhynchus mykiss*) muscle proteins by preslaughter activity. *J. Agric. Food Chem.* **2006**, *54*, 2997−3001.
(21) Vasiliou, V.; Brocker, C.; Lassen, N.; Estey, T.; Pappa, A.; Cantore, M.; Orlova, V. V.; Chavakis, T.; Kavanagh, K. L.; Oppermann, U. Aldehyde dehydrogenase 7A1 (ALDH7A1) is a novel enzyme involved in cellular defense against hyperosmotic stress. *J. Biol. Chem.* **2010**, *285*, 18452−18463.
(22) Jia, X.; Hollung, K.; Therkildsen, M.; Hildrum, K. I.; Bendixen, E. Proteome analysis of early post-mortem changes in two bovine muscle types: M. longissimus dorsi and M. semitendinosis. *Proteomics* **2006**, *6*, 936−44.
(23) El-Deiry, W. S.; Corn, P. G.; McDonald, E. R.; Herman, J. G. Tat-binding protein-1, a component of the 26S proteasome, contributes to the E3 ubiquitin ligase function of the von Hippel-Lindau protein. *Nat. Genet.* **2003**, *35*, 229−237.